Report

Cell Reports

Protein Dimerization Generates Bistability in Positive Feedback Loops

Graphical Abstract

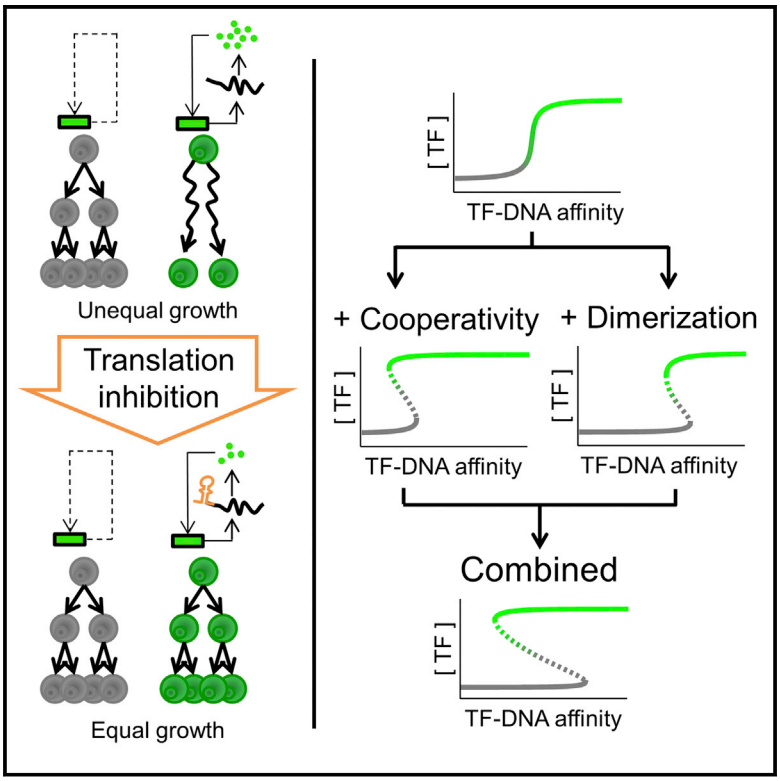

Authors

Chieh Hsu, Vincent Jaquet, Mumun Gencoglu, Attila Becskei

Correspondence

attila.becskei@unibas.ch

In Brief

Using RNA stem loops to attenuate translation rates, Hsu et al. designed synthetic feedback loops in yeast to study the sources of bistability. They show that cooperative binding of a transcription factor to its promoter or its dimerization generates bistability. Bistability is particularly robust when the dimerizing transcription factor binds to the promoter cooperatively.

Highlights

- RNA stem loops tune translation rates over two orders of magnitude
- Positive feedback loops with reduced translation generate bistable cell fates
- Dimerizing transcription factors generate bistability without cooperative binding

Hsu et al., 2016, Cell Reports *16*, 1–7
August 2, 2016
http://dx.doi.org/10.1016/j.celrep.2016.06.072

CellPress

Please cite this article in press as: Hsu et al., Protein Dimerization Generates Bistability in Positive Feedback Loops, Cell Reports (2016), http://dx.doi.org/10.1016/j.celrep.2016.06.072

Cell Reports
Report

Protein Dimerization Generates Bistability in Positive Feedback Loops

Chieh Hsu,[1,2,3] Vincent Jaquet,[1,3] Mumun Gencoglu,[1] and Attila Becskei[1,*]
[1]Biozentrum, University of Basel, Klingelbergstrasse 50/70, 4056 Basel, Switzerland
[2]School of Biosciences, University of Kent, Canterbury, Kent CT2 7NJ, UK
[3]Co-first author
*Correspondence: attila.becskei@unibas.ch
http://dx.doi.org/10.1016/j.celrep.2016.06.072

SUMMARY

Bistability plays an important role in cellular memory and cell-fate determination. A positive feedback loop can generate bistability if it contains ultrasensitive molecular reactions. It is often difficult to detect bistability based on such molecular mechanisms due to its intricate interaction with cellular growth. We constructed transcriptional feedback loops in yeast. To eliminate growth alterations, we reduced the protein levels of the transcription factors by tuning the translation rates over two orders of magnitude with designed RNA stem loops. We modulated two ultrasensitive reactions, homodimerization and the cooperative binding of the transcription factor to the promoter. Either of them is sufficient to generate bistability on its own, and when acting together, a particularly robust bistability emerges. This bistability persists even in the presence of a negative feedback loop. Given that protein homodimerization is ubiquitous, it is likely to play a major role in the behavior of regulatory networks.

INTRODUCTION

Bistability, the persistence of two alternative stable-activity states under identical conditions, can uphold alternative cell fates and differentiation states, store cellular memory of past stimuli, and enhance adaptation in organisms ranging from bacteria to mammals (Angel et al., 2011; Arnoldini et al., 2014; Bouchoucha et al., 2013; Chickarmane et al., 2009; Park et al., 2012).

Positive feedback is a necessary, but not sufficient, condition for bistability in a gene regulatory network. The second requirement is that the feedback loop contains reactions such as cooperative binding, sequestration by inhibitor molecules, and multiple phosphorylation of a protein by a kinase (Chen and Arkin, 2012; Ferrell and Ha, 2014; Májer et al., 2015; Shopera et al., 2015; Thomson and Gunawardena, 2009). These reactions display a sigmoidal, switch-like nonlinear response, also termed ultrasensitive response. Without ultrasensitive responses, a feedback loop can have only a single steady-state expression level, i.e., the system is monostable.

In transcriptional regulation, dimerization and cooperative binding of a transcription factor are expected to be common sources of ultrasensitivity (Buchler and Louis, 2008). Most transcription factors bind to DNA as dimers, and binding can be cooperative when more than one binding site is present in a promoter (Becskei et al., 2005). Despite the ubiquity of protein homodimerization, its ability to generate bistability remained elusive.

The difficulty to identify the sources of bistability may be explained by the effect of the feedback loop on cell growth. In positive feedback loops, the transcription factors are often expressed at high levels; therefore, they can sequester mediators of transcription (Becskei et al., 2001; Kelleher et al., 1990). This results in squelching of global gene expression, which reduces cellular growth and alters the behavior of networks. Even more, growth alterations rather than ultrasensitivity in the feedback can generate bistability (Brophy and Voigt, 2014; Tan et al., 2009).

In this work, we illustrated a design principle to tackle this difficulty with synthetic feedback loops. We show that alteration of the cell growth caused by overexpression of the transcription factor can be circumvented by using RNA stem loops to adjust translation rates. After translation rate adjustment, we show that either of the two ultrasensitive reactions, cooperative binding to the promoter or homodimerization, can support bistability. When they were both present, a particularly robust bistability emerged.

RESULTS

Design of Synthetic Loop and Control Elements

Synthetic positive feedback loops were created by placing the gene encoding the transcription factor rtTA (reverse tetracycline transactivator) under the control of a promoter containing *tet* operators and inserted into the chromosome of the yeast *S. cerevisiae* (Table S1). rtTA is composed of the bacterial rTetR DNA-binding domain and the VP16 activation domain; rtTA binds to the *tet* operators only in dimeric form (Kamionka et al., 2006). The ligand doxycycline enables rtTA to bind to *tet* operators; thus, the affinity of rtTA binding to DNA was adjusted by the ligand concentration (Figure 1A).

Please cite this article in press as: Hsu et al., Protein Dimerization Generates Bistability in Positive Feedback Loops, Cell Reports (2016), http://dx.doi.org/10.1016/j.celrep.2016.06.072

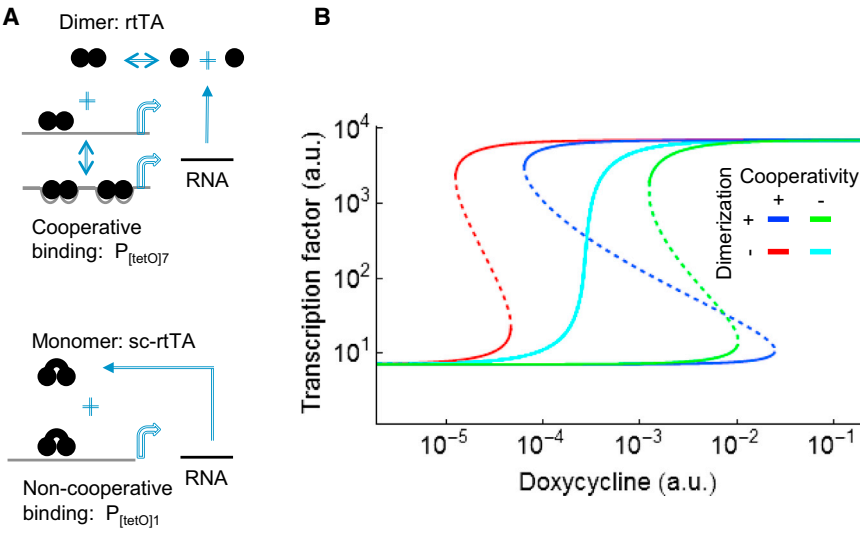

Figure 1. Design and Models of Feedback Loops with Cooperative Binding and Homodimerization

(A) Feedback loop design. Two examples are shown for the feedback loops: the loop with two ultrasensitive reactions: cooperative binding and dimerization (upper panel) and the loop without ultrasensitive reaction (lower panel).

(B) The effect of cooperative binding and protein dimerization on the steady-state levels in the feedback loop as a function of the binding strength of transcription factor to DNA, as indicated by the doxycycline concentration. When three (one unstable and two stable) steady-state expression levels are found in a certain range of doxycycline concentration, the system is bistable. The Hill coefficient of the cooperative binding was 1.45, and the equilibrium dissociation constant (K_D) for dimerization was 1,000 (in concentration units identical to that of the transcription factor).

See also Supplemental Information.

To study the effect of dimerization, we compared the original dimeric rtTA with a monomeric form. To create this monomeric form, two rTetR DNA-binding domains were fused. The resulting single-chain monomer (sc-rtTA) alone is capable of binding to the palindromic operators, eliminating the ultrasensitive dimerization reaction (Zhou et al., 2007). To study the effect of cooperativity, we changed the number of *tet* operators in the promoter. The binding of rtTA to a single *tet* operator is non-cooperative, while binding to seven operators in a promoter is cooperative (Becskei et al., 2005) (Figure 1A).

If a transcriptional positive feedback loop incorporates cooperative binding or dimerization, bistability is expected in a certain doxycycline concentration range. This range is expected to be broader when both reactions are present (Figure 1B). To test the individual and joint effect of these mechanisms, we constructed all four variants of the feedback loop. We measured the activity of a feedback loop with a GFP reporter controlled by a promoter with *tet* operators (Figure 2A).

Growth Alteration by Overexpression of the Transcription Factor Caused Atypical Hysteresis

We evaluated bistability with hysteresis experiments that test whether the system activity depends on the initial condition, i.e., on its history. Pre-cultures with either low or high expression states of rtTA were prepared, which defines the initial conditions, and the cells were further cultured at different doxycycline concentrations. The range of doxycycline concentrations at which the expression in each culture remains close to the respective initial condition—and, therefore, different from each other—defines the range of hysteresis. To adjust the initial condition, we integrated an inducible rtTA construct into the chromosome. Its expression was controlled by the P_{GAL} promoter. By a transient exposure of cells to galactose, the rtTA is expressed at a high level to establish the high initial condition (Figure 2A).

When hysteresis experiments were performed for the cooperative-dimeric feedback loop, the cell expression deviated markedly from the initial state. Even more, the high expression level was observed only in cells with the low initial condition, while cells with the high initial condition failed to maintain high expression (Figure 2B). This is the exact opposite of the conventional hysteresis behavior. Similarly unusual was the behavior of the non-cooperative-dimeric feedback loop (Figure S1A).

We suspected that the high expression of the rtTA affects the cell growth and alters the system's behavior. Indeed, a reduced growth rate was observed at a high doxycycline concentration at which the system should have been fully activated (Figure 2C).

Translation Rate Tuning with RNA Stem Loop and Feedback Loop Optimization

To eliminate the growth rate alteration, we lowered the protein expression level by decreasing the translation rate with RNA stem loop. A stem loop upstream of the start codon is expected to reduce the translation rate by preventing ribosome from initiating the translation. When a stem loop with a stem containing six G-C base pairs (or $SL_{6[AT]0}$) (Beelman and Parker, 1994) was incorporated into the cooperative-dimeric feedback loop, no growth defect was detected anymore, and the growth rates in all conditions were identical (Figure 2C). However, the reporter gene expression was very weak, indicating that the rtTA protein concentration was too low to activate the system (Figure 2B).

To reach a sufficient protein expression level without causing growth defect, we synthesized stem loops and measured their respective translation rates. The strength of translation inhibition of the stem loop depends on its structure. We weakened the stem structure of the initial $SL_{6[AT]0}$ by shortening the stem length to five base pairs and by increasing the proportion of A-T base pairs. The absolute translation rate was calculated from the steady-state expression levels of RNA and protein and the protein decay rate. The molecule numbers of RNAs and proteins were measured with single-molecule fluorescence in situ hybridization (smFISH) and mass spectrometry, respectively (Experimental Procedures; Supplemental Experimental Procedures). We obtained a variety of stem loops that can tune the translation rate over two orders of magnitude (Figure 3A). We also checked how robust the stem loops behave in different sequence context. For this purpose, we inserted these stem loops upstream of the

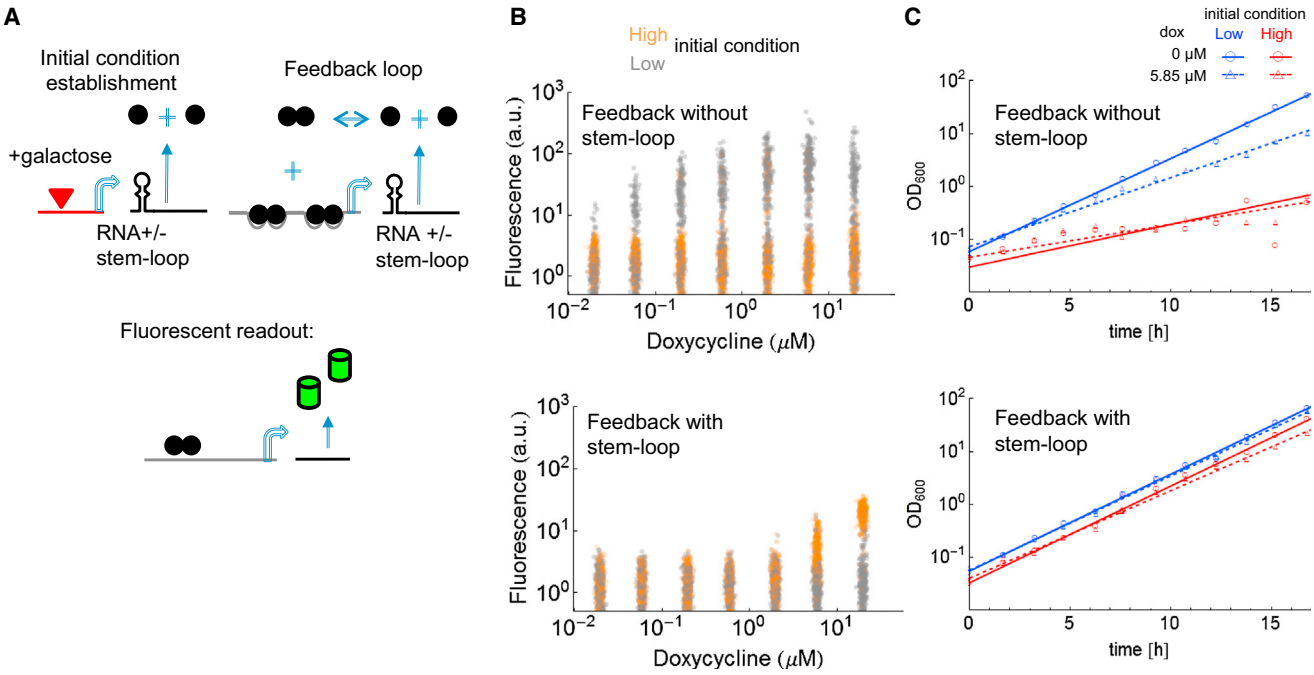

Figure 2. Hysteresis Experiments with Altered Growth Rates

(A) Circuit design. The activity of the cooperative-dimeric loop is reported with a GFP reporter (green) under $P_{[tetO]2}$ and measured with flow cytometry. High and low initial conditions (transcription factor expression levels) were established with the P_{GAL} promoter (red), which can be induced transiently by galactose. Expression of P_{GAL} is independent of the doxycycline-inducible promoters. To reduce the expression level of the transcription factor, a stem loop was incorporated in the RNA upstream of the start codon.

(B) The hysteresis experiment of the dimeric-cooperative loop without (upper panel) or with (lower panel) incorporated non-optimized RNA stem loop ($SL_{6[AT]0}$) to modulate translation. Cells with the low (gray dots) or the high (orange dots) initial condition were grown at the indicated doxycycline concentration for 24 hr.

(C) Growth curves of cells containing the cooperative-dimeric loop without (upper panel) or with (lower panel) incorporated RNA stem loop under indicated initial conditions and doxycycline concentrations during the hysteresis experiments.

See also Figure S1.

start codon of a fluorescent reporter gene, YFP (yellow fluorescent protein). The decrease of fluorescence with increasing stem-loop strength was very similar to that observed for the absolute translation rates of the rtTA mRNA (Figure 3A).

A specific stem loop was selected for each feedback construct in order to eliminate growth alterations without reducing protein concentration to below the level required to activate the feedback loops (Figures 3B and S1).

The decay rates of the rtTA and the sc-rtTA proteins were similar, with half-lives of 79 and 83 min, respectively (Figure 3C). The similar decay rates of the two proteins permit their consistent comparison of the feedback loops in the hysteresis experiments.

Homodimerization and Cooperativity Generate Bistability

With the optimized feedback loops, we observed classical hysteresis behavior: cells with the high initial condition had higher or equal expression than cells with the low initial condition (Figure 4A). The non-cooperative-monomeric loop displayed no hysteresis, the expressions of cells were very similar, independent of the initial condition. When one of the ultrasensitive reactions—either cooperative binding or dimerization—was included in the feedback loop, bistability emerged. The non-cooperative-dimeric loop displayed hysteresis over one order of magnitude of doxycycline concentration, which is broader than that for the cooperative-monomeric circuit. Combining the two mechanisms, a particularly broad range of hysteresis emerged. The cells with a high initial condition remained in the high expression state; and cells with the low initial condition remained in the low expression state over at least two orders of magnitude of doxycycline concentrations. This represents a robust form of cellular memory. These results confirm the expectations from the theoretical model (Figure 1B).

Negative Feedback Reduces the Robustness of Bistability

Positive feedback loops are often combined with negative ones. This combination is expected to reduce the bistable range (Tian et al., 2009). To extend the cooperative-dimeric positive feedback loop with a negative loop, additional *tet* operators were integrated downstream of the TATA box in the promoter (Figure 4B). The binding of rtTA to these two *tet* operators was shown to repress transcription. At low doxycycline concentration, the binding to the seven upstream *tet* operators activates gene expression, while at higher doxycycline concentration, repression predominates. Consequently, the promoter displays a bell-shaped response (Figure S2A) (Buetti-Dinh et al., 2009).

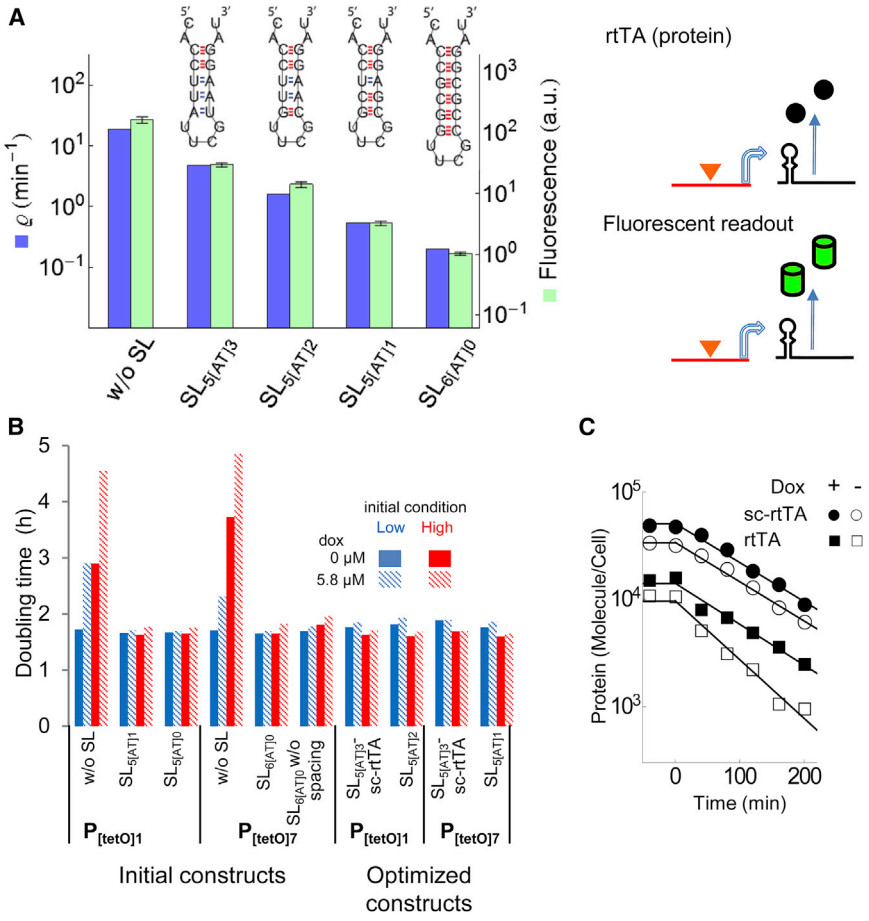

Figure 3. Optimization of Protein Expression Levels with Various RNA Stem Loops

(A) Translation rates of mRNAs with different stem loops. Stem loops with different lengths and AT/GC contents were incorporated upstream of the start codon of the transcription factor rtTA or a fluorescence reporter under control of the P_{GAL} promoter as indicated. The absolute translation rates and the relative fluorescence signals were measured. The following values were obtained for the translation rates (left to right): 18.6, 4.8, 1.6, 0.54, and 0.2 min^{-1}.

(B) The effect of stem loop optimization on growth in different feedback constructs. The growth rates of cells containing the indicated feedback loops with various RNA stem loops were determined by linear regression under different initial conditions (init.) and doxycycline (dox) concentrations during the hysteresis experiments.

(C) The decay rates of proteins were measured by shut-off assay (Supplemental Experimental Procedures). The fitted decay rate constants of rtTA protein are 0.0126 ± 0.0009 and 0.0088 ± 0.0006 min^{-1} (estimate ± SE) with and without 20 μM dox, respectively. Both values are 0.0084 ± 0.0004 min^{-1} for sc-rtTA.

See also Supplemental Experimental Procedures and Figure S1.

In theory, a feedback loop with this promoter has a narrower range of bistability compared to the cooperative-dimeric feedback loop (Figure S2B). Furthermore, the higher expression state is predicted to be lower. This may explain why no growth alteration was observed and no stem loop was needed for this feedback loop. The range of hysteresis of this dual positive-negative feedback system was narrower than that of the corresponding positive feedback (cooperative-dimeric). However, it was still wider than the hysteresis range of loops with a single ultrasensitive reaction step (Figure 4C), which indicates again the robustness of the bistability when cooperative binding and homodimerization act together.

DISCUSSION

We observed bistability due to ultrasensitive molecular mechanisms only when cell growth alterations due to the feedback loops were eliminated. This behavior stands in contrast to those systems where bistability arises due to the interaction of the feedback loop and cellular growth. For example, regulators have been identified that slow down cell growth, which then establishes a positive feedback loop to control cell differentiation (Chiodini et al., 2013; Kueh et al., 2013; Tan et al., 2009). Coupling of feedback loops with growth rate is likely to represent an important phenomenon, since differentiating cells that enter distinct cell lineages often have disparate growth rates (Cheeseman et al., 2014). In our system, the reduction of cell growth was due to the squelching of gene expression of a highly expressed activator. Interestingly, endogenous transcriptional activators are also known that can repress gene expression by squelching (Guertin et al., 2014; Schmidt et al., 2015).

To eliminate growth alterations, we reduced protein concentration by translational inhibition. Interestingly, the range of inhibition was quite narrow that permitted the activation of the feedback loops without affecting growth rate. This requirement was met by the stem-loops we created because it was possible to modulate the translation rate over a broad dynamic range, which makes them an ideal tool in systems and synthetic biology (Chappell et al., 2015; McKeague et al., 2016). Furthermore, the stem loops reduce the translation of different proteins similarly (Figure 3A). The absolute translation rate without stem-loop was around 20 min^{-1}, while it was around 0.2 min^{-1} with the stem loop having the highest GC content. This means that, on average, 20 protein molecules are translated from an RNA molecule per minute without the stem loop. To our knowledge, no absolute translation rate has been measured in yeast, but a comparison of genome-wide studies on yeast mRNA, protein abundances, and protein half-lives yields similar estimates for the average translation rate (23 min^{-1}) (Belle et al., 2006; To and Maheshri, 2010).

The loop with the monomeric transcriptional activator and a single site in the promoter lacks any ultrasensitive reaction, and bistability was absent. By adding either dimerization or

Please cite this article in press as: Hsu et al., Protein Dimerization Generates Bistability in Positive Feedback Loops, Cell Reports (2016), http://dx.doi.org/10.1016/j.celrep.2016.06.072

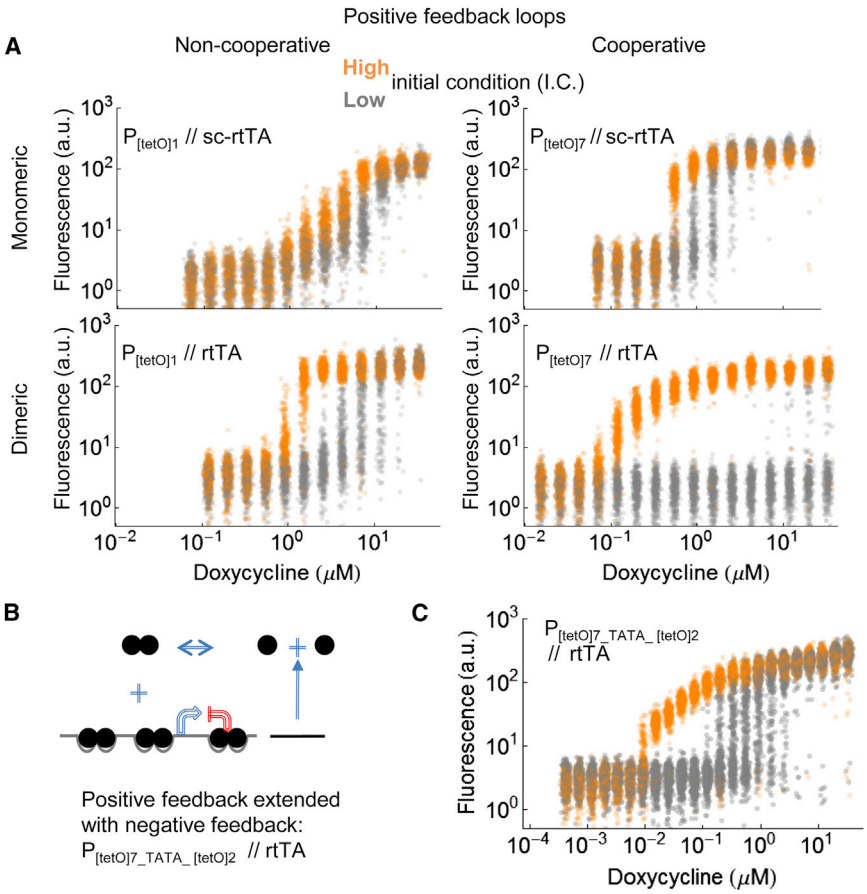

Figure 4. Hysteresis in Feedback Circuits Incorporating Protein Homodimerization or Cooperative Binding to the Promoter

(A) Hysteresis experiments with circuits with optimized stem loops as indicated in Figure 3. Cells with the low (gray dots) or the high (orange dots) initial condition were grown at the indicated doxycycline concentration for 24 hr.

(B and C) Hysteresis in dual positive-negative feedback based on the cooperative-dimeric circuit. The negative feedback was established by inserting transcription factor binding sites downstream of the TATA box site in the promoter, which inhibits transcription (red) (B). Hysteresis experiments were performed with the cells containing this feedback construct without RNA stem loop for 24 hr.

See also Figure S2.

cooperative binding to the circuit, we can assess their contribution to bistability separately. In principle, the following two feedback loops can generate identical bistable ranges: (1) the dimeric transcription factor that binds to a single site in the DNA, provided the concentration of the protein is less than its dimerization equilibrium dissociation constant; and (2) a monomeric factor that binds cooperatively to multiple sites in a promoter with a Hill coefficient of 2 (Májer et al., 2015). However, the binding of rtTA to the cooperative promoter has a Hill coefficient of 1.45 (Becskei et al., 2005). Thus, the larger potential ultrasensitivity of dimerization may explain why bistability had a broader range in the presence of homodimerization than in the presence of cooperative binding (Figure 4A).

Bistability based on dimerization reactions has eluded detection, although the majority of proteins di- or multimerize across all domains of life (Lynch, 2012; Marianayagam et al., 2004). This apparent paradox may have several reasons. First, it is difficult to separate the specific effect of dimerization exactly, because it is ubiquitous. In typical networks, dimerization is combined with other, more evident, ultrasensitive reactions exemplified by sequestration or cooperative binding. Second, a dimerization reaction becomes ultrasensitive and, thus, can support bistability only if the protein concentration is low enough (Buchler and Louis, 2008; Májer et al., 2015). The reduced concentration of the dimerizing protein in our circuits is likely to have facilitated the emergence of bistability.

Positive feedback loops have been uncovered in a broad range of regulatory processes (Chiodini et al., 2013; Kueh et al., 2013; Park et al., 2012). Our study provides clues on how to detect the bistability due to homodimerization in feedback loops. It has the potential to contribute to other dynamical behaviors, such as oscillation and pattern formation (Ferrell and Ha, 2014). Given the ubiquity of homodimerization, it is likely that it plays an important role in these processes as well.

EXPERIMENTAL PROCEDURES

Design of Synthetic Circuits and Yeast Strains

Each feedback strain contained a feedback circuit, a fluorescent reporter construct ($P_{[tetO]2}$- yEGFP), and a P_{GAL}-rtTA/sc-rtTA expression cassette. The P_{GAL}-rtTA/sc-rtTA expression cassette was utilized to generate the high initial condition by adding 0.5% galactose for the hysteresis experiments. Galactose activates expression driven by the P_{GAL} promoter through the endogenous Gal4p. The P_{GAL} is a modified version of P_{GAL1} (denoted as P_GAL1UAS-CYC1c in Table S1).

All yeast strains are derivatives of *S. cerevisiae* W303 (Table S1). All genetic constructs were integrated into the chromosome with a single copy, with the exception of the $P_{[tetO]2}$-GFP construct, which has three copies. To minimize the position effect, genes with promoters containing *tet* operators were integrated to the *ura3* locus, and those with P_{GAL} were integrated to the *ade2* locus.

The synthetic genetic components share a common core promoter and transcriptional terminator of *CYC1*, unless otherwise specified. The *CYC1* core promoter, *CYC1*c, is a 137-bp sequence upstream of the start codon of *CYC1*, which contains the TATA box. The upstream activation sequences (UASs), including tetO and *GAL1*, were attached to this core promoter sequence. The Mig1p-binding site in the UAS from *GAL1* was inactivated. A BamHI site was introduced between *CYC1*c and the start codon.

The stem loop sequences were derived from the following $SL_{6[AT]0}$ sequence, 5′-CCGCGGTTCGCCGCGG-3′ (Beelman and Parker, 1994): 5′-CCGCGTTCGCGCGG-3′ ($SL_{5[AT]0}$), 5′-CCTCGTTCGCGAGG-3′ ($SL_{5[AT]1}$), 5′-CCTTGTTCGCAAGG-3′ ($SL_{5[AT]2}$) and 5′-CCTTATTCGTAAGG-3′ ($SL_{5[AT]3}$). The stem loops were inserted into the *CYC1c* region of the promoter with a 13-bp spacing before the start codon. The sequences upstream and downstream of the stem loop were ATTACCGGATCA and ATTCGGGggatccATG; the ATG at the 3′ end is the start codon, and ggatcc is a BamHI recognition site. The design of the stem loop was checked by the free energy calculated from the Vienna RNA Websuite (Gruber et al., 2008).

For the rtTA protein, the S2 version of the reverse tetracycline transactivator was used (Becskei et al., 2005). sc-rtTA is a chain of two connected tetRs followed by a single VP16 activation domain. The F86Y and G138D mutations (FYGD) were introduced in both tetRs to enhance transcription activity (Zhou et al., 2007). To reduce recombination within the sc-rtTA sequence, an extra *Hin*DIII site was introduced to the rtTA sequence (silent mutation, position 102 in ORF [open reading frame]), and the sequence of a codon-humanized FYGD version of tetR (Zhou et al., 2007) containing the linker was inserted into the *Hin*DIII site. The *Stu*I and BamHI sites in the ORF sequence were inactivated.

Hysteresis Experiment

General growth conditions and flow cytometry are described in the Supplemental Experimental Procedures. Low and high expression states were created as initial conditions, termed low and high initial conditions. The high initial condition was generated by culturing cells overnight with 2 μM doxycycline and 0.5% galactose, while no inducers were added for the low initial condition. Subsequently, the cultures were transferred to fresh media starting at an optical density at 600 nm (OD_{600}) of 0.2 and grown for additional 4 hr. These cells were then inoculated into media containing a doxycycline concentration range so that cells with different initial conditions were grown in identical conditions. There was no need to wash the cells prior to inoculation to remove the inducers, since the inoculum was diluted at least 1,000 times. The initial culture density was adjusted so that the OD_{600} reaches values between 0.6 and 1.0 at 24 hr.

Translation Rate Constant Determination

The translation rate was determined in steady-state conditions. The protein concentration $[P]$ is governed by:

$$\frac{d[P]}{dt} = \rho[mRNA] - \delta_P[P].$$

δ_P is the protein decay rate constant; ρ is the translation rate constant; and $[P]$ and $[mRNA]$ represent the copy numbers of protein and mRNA in a cell, respectively.

Therefore, ρ is equal to $(\delta_P[P]/[mRNA])$ in steady state.

The decay rate constant of the protein was determined as explained in the Supplemental Information. To determine the effect of stem loops on translation, strains (indicated by "Translation rate determination" in the Function column of Table S1) were constructed that express rtTA with different stem loops under the control of GEV. GEV also binds to and activates the GAL promoters, but only in the presence of estradiol. The RNA expression can be tuned over a broad range by adjusting the estradiol concentration (Bonde et al., 2014). In this way, it was possible to express rtTA without growth alterations. Cells were grown for 24 hr with 10 nM or 100 nM estradiol to reach steady-state expression. The culture was split for the quantification of RNA with qPCR and protein with absolute protein quantification by mass spectrometry. To convert the mRNA data measured by qPCR to absolute counts, we measured the ratio of the RNA levels obtained by qPCR to that by smFISH (Supplemental Experimental Procedures). The reported translation rates are averages calculated from the two steady-state expression levels induced with 10 nM or 100 nM estradiol.

The absolute translation rates were verified by assessing relative translation efficiencies with fluorescent reporters, in which the same stem loops were inserted. These haploid strains, indicated in Table S1 with "translation efficiency strains," were incubated with 80 nM estradiol for 24 hr to reach steady-state expression levels of the fluorescent reporter.

Mathematical Modeling

Details are provided in the Supplemental Information.

SUPPLEMENTAL INFORMATION

Supplemental Information includes Supplemental Experimental Procedures, two figures, and one table and can be found with this article online at http://dx.doi.org/10.1016/j.celrep.2016.06.072.

AUTHOR CONTRIBUTIONS

A.B. designed the project. M.G. performed the proteomics measurements and the initial experiments with the dual-feedback constructs. C.H. and V.J. performed all the other experiments and data analysis. A.B., C.H., and V.J. wrote the paper.

ACKNOWLEDGMENTS

We thank A. Das for the sc-rtTA plasmid; S. Voegeli, J. Kelemen, and S. Scherrer for help with plasmid construction and sequencing; J. Zankl for help with the flow cytometry; and A. Schmidt for help with proteomic measurements. This work was supported by grants from the Swiss National Foundation, the StoNets RTD, and IPhD from SystemsX. C.H. was a Long-Term Fellow of the Human Frontier Science Program.

Received: September 24, 2015
Revised: May 22, 2016
Accepted: June 16, 2016
Published: July 14, 2016

REFERENCES

Angel, A., Song, J., Dean, C., and Howard, M. (2011). A Polycomb-based switch underlying quantitative epigenetic memory. Nature *476*, 105–108.

Arnoldini, M., Vizcarra, I.A., Peña-Miller, R., Stocker, N., Diard, M., Vogel, V., Beardmore, R.E., Hardt, W.D., and Ackermann, M. (2014). Bistable expression of virulence genes in salmonella leads to the formation of an antibiotic-tolerant subpopulation. PLoS Biol. *12*, e1001928.

Becskei, A., Séraphin, B., and Serrano, L. (2001). Positive feedback in eukaryotic gene networks: cell differentiation by graded to binary response conversion. EMBO J. *20*, 2528–2535.

Becskei, A., Kaufmann, B.B., and van Oudenaarden, A. (2005). Contributions of low molecule number and chromosomal positioning to stochastic gene expression. Nat. Genet. *37*, 937–944.

Beelman, C.A., and Parker, R. (1994). Differential effects of translational inhibition in cis and in trans on the decay of the unstable yeast MFA2 mRNA. J. Biol. Chem. *269*, 9687–9692.

Belle, A., Tanay, A., Bitincka, L., Shamir, R., and O'Shea, E.K. (2006). Quantification of protein half-lives in the budding yeast proteome. Proc. Natl. Acad. Sci. USA *103*, 13004–13009.

Bonde, M.M., Voegeli, S., Baudrimont, A., Séraphin, B., and Becskei, A. (2014). Quantification of pre-mRNA escape rate and synergy in splicing. Nucleic Acids Res. *42*, 12847–12860.

Bouchoucha, Y.X., Reingruber, J., Labalette, C., Wassef, M.A., Thierion, E., Desmarquet-Trin Dinh, C., Holcman, D., Gilardi-Hebenstreit, P., and Charnay, P. (2013). Dissection of a Krox20 positive feedback loop driving cell fate choices in hindbrain patterning. Mol. Syst. Biol. *9*, 690.

Brophy, J.A., and Voigt, C.A. (2014). Principles of genetic circuit design. Nat. Methods *11*, 508–520.

Buchler, N.E., and Louis, M. (2008). Molecular titration and ultrasensitivity in regulatory networks. J. Mol. Biol. *384*, 1106–1119.

Buetti-Dinh, A., Ungricht, R., Kelemen, J.Z., Shetty, C., Ratna, P., and Becskei, A. (2009). Control and signal processing by transcriptional interference. Mol. Syst. Biol. *5*, 300.

Chappell, J., Watters, K.E., Takahashi, M.K., and Lucks, J.B. (2015). A renaissance in RNA synthetic biology: new mechanisms, applications and tools for the future. Curr. Opin. Chem. Biol. *28*, 47–56.

Cheeseman, B.L., Zhang, D., Binder, B.J., Newgreen, D.F., and Landman, K.A. (2014). Cell lineage tracing in the developing enteric nervous system: superstars revealed by experiment and simulation. J. R. Soc. Interface *11*, 20130815.

Chen, D., and Arkin, A.P. (2012). Sequestration-based bistability enables tuning of the switching boundaries and design of a latch. Mol. Syst. Biol. *8*, 620.

Chickarmane, V., Enver, T., and Peterson, C. (2009). Computational modeling of the hematopoietic erythroid-myeloid switch reveals insights into cooperativity, priming, and irreversibility. PLoS Comput. Biol. *5*, e1000268.

Chiodini, F., Matter-Sadzinski, L., Rodrigues, T., Skowronska-Krawczyk, D., Brodier, L., Schaad, O., Bauer, C., Ballivet, M., and Matter, J.M. (2013). A positive feedback loop between ATOH7 and a Notch effector regulates cell-cycle progression and neurogenesis in the retina. Cell Rep. *3*, 796–807.

Ferrell, J.E., Jr., and Ha, S.H. (2014). Ultrasensitivity part III: cascades, bistable switches, and oscillators. Trends Biochem. Sci. *39*, 612–618.

Gruber, A.R., Lorenz, R., Bernhart, S.H., Neuböck, R., and Hofacker, I.L. (2008). The Vienna RNA websuite. Nucleic Acids Res. *36*, W70–W74.

Guertin, M.J., Zhang, X., Coonrod, S.A., and Hager, G.L. (2014). Transient estrogen receptor binding and p300 redistribution support a squelching mechanism for estradiol-repressed genes. Mol. Endocrinol. *28*, 1522–1533.

Kamionka, A., Majewski, M., Roth, K., Bertram, R., Kraft, C., and Hillen, W. (2006). Induction of single chain tetracycline repressor requires the binding of two inducers. Nucleic Acids Res *34*, 3834–3841.

Kelleher, R.J., 3rd, Flanagan, P.M., and Kornberg, R.D. (1990). A novel mediator between activator proteins and the RNA polymerase II transcription apparatus. Cell *61*, 1209–1215.

Kueh, H.Y., Champhekar, A., Nutt, S.L., Elowitz, M.B., and Rothenberg, E.V. (2013). Positive feedback between PU.1 and the cell cycle controls myeloid differentiation. Science *341*, 670–673.

Lynch, M. (2012). The evolution of multimeric protein assemblages. Mol. Biol. Evol. *29*, 1353–1366.

Májer, I., Hajihosseini, A., and Becskei, A. (2015). Identification of optimal parameter combinations for the emergence of bistability. Phys. Biol. *12*, 066011.

Marianayagam, N.J., Sunde, M., and Matthews, J.M. (2004). The power of two: protein dimerization in biology. Trends Biochem. Sci. *29*, 618–625.

McKeague, M., Wong, R.S., and Smolke, C.D. (2016). Opportunities in the design and application of RNA for gene expression control. Nucleic Acids Res. *44*, 2987–2999.

Park, B.O., Ahrends, R., and Teruel, M.N. (2012). Consecutive positive feedback loops create a bistable switch that controls preadipocyte-to-adipocyte conversion. Cell Rep. *2*, 976–990.

Schmidt, S.F., Larsen, B.D., Loft, A., Nielsen, R., Madsen, J.G., and Mandrup, S. (2015). Acute TNF-induced repression of cell identity genes is mediated by NFκB-directed redistribution of cofactors from super-enhancers. Genome Res. *25*, 1281–1294.

Shopera, T., Henson, W.R., Ng, A., Lee, Y.J., Ng, K., and Moon, T.S. (2015). Robust, tunable genetic memory from protein sequestration combined with positive feedback. Nucleic Acids Res. *43*, 9086–9094.

Tan, C., Marguet, P., and You, L. (2009). Emergent bistability by a growth-modulating positive feedback circuit. Nat. Chem. Biol. *5*, 842–848.

Thomson, M., and Gunawardena, J. (2009). Unlimited multistability in multisite phosphorylation systems. Nature *460*, 274–277.

Tian, X.J., Zhang, X.P., Liu, F., and Wang, W. (2009). Interlinking positive and negative feedback loops creates a tunable motif in gene regulatory networks. Phys. Rev. E Stat. Nonlin. Soft Matter Phys. *80*, 011926.

To, T.L., and Maheshri, N. (2010). Noise can induce bimodality in positive transcriptional feedback loops without bistability. Science *327*, 1142–1145.

Zhou, X., Symons, J., Hoppes, R., Krueger, C., Berens, C., Hillen, W., Berkhout, B., and Das, A.T. (2007). Improved single-chain transactivators of the Tet-On gene expression system. BMC Biotechnol. *7*, 6.